ORIGINAL RESEARCH

Altered resting-state functional networks in patients with premenstrual syndrome: a graph-theoretical based study

Chengxiang Liu[1,2] · Chunmei Xuan[3] · Jiayu Wu[1,2] · Shasha Li[3] · Guang Yang[1,2] · Ruiqing Piao[1,2] · Gaoxiong Duan[3] · Demao Deng[4] · Peng Liu[1,2]

Abstract

Premenstrual syndrome (PMS) is a menstrual cycle-related disorder. Previous studies have indicated alterations of brain functional connectivity in PMS patients. However, little is known about the overall organization of brain network in PMS patients. Functional magnetic resonance imaging data deriving from 20 PMS patients and 21 healthy controls (HCs). Pearson correlation between mean time-series was used to estimate connectivity matrix between each paired regions of interest, and the connectivity matrix for each participant was then binarized. Graph theory analysis was applied to assess each participant's global and local topological properties of brain functional network. Correlation analysis was performed to evaluate relationships between the daily rating of severity of problems (DRSP) and abnormal network properties. PMS patients had lower small-worldness values than HCs. PMS-related alterations of nodal properties were mainly found in the posterior cingulate cortex, precuneus and angular gyrus. The PMS-related abnormal connectivity components were mainly associated with the thalamus, putamen and middle cingulate cortex. In the PMS group, the DRSP score were negatively correlated with the area under the curves of nodal local efficiency in the posterior cingulate cortex. Our study suggests that the graph-theory method may be one potential tool to detect disruptions of brain connections and may provide important evidence for understanding the PMS from the disrupted network organization perspective.

Keywords Brain functional network · Topological analysis · Premenstrual syndrome · Functional magnetic resonance imaging

Chengxiang Liu and Chunmei Xuan these authors equally contributed to this manuscript

✉ Demao Deng
demaodeng@163.com

✉ Peng Liu
liupengphd@gmail.com

[1] Life Science Research Center, School of Life Science and Technology, Xidian University, Xi`an 710071, Shaanxi, China

[2] Engineering Research Center of Molecular and Neuro Imaging Ministry of Education, School of Life Science and Technology, Xidian University, Xi`an 710071, Shaanxi, China

[3] Department of Radiology, First Affiliated Hospital, Guangxi University of Chinese Medicine, Nanning, Guangxi, China

[4] Department of Radiology, the People's Hospital of Guangxi Zhuang Autonomous Region, Nanning 530021, Guangxi, China

Introduction

Premenstrual syndrome (PMS) is used to describe physical, affective, behavioral, and cognitive symptoms that occur cyclically during the luteal phase of the menstrual cycle and this symptoms are relieved gradually in the first few days of menstruation (Le et al., 2020; Ryu & Kim, 2015; Tolossa & Bekele, 2014). According to previous studies that PMS occurs in 30–40% of reproductive-age females (Le et al., 2020). The major symptoms of PMS are: aches, tired, anxiety, depressive, irritability, hypersomnia and decreased interest in activities and reduces women's willpower, significantly affecting their social interactions and normal life (Wu et al. 2016a, b; Quintana-Zinn et al. 2017; Liu et al. 2017a, b; Bu et al. 2019). A comprehensive neurobiological understanding of menstrual reactivity is critical for identifying the neuropathology and developing appropriate treatments to reduce the impact of PMS.

Recent neuroimaging studies of PMS patients have disclosed the resting-state brain functional networks undergoes maladaptive or adaptive reorganizations. Previous studies demonstrated that PMS patients had aberrant activity within the default mode network (DMN) (De Bondt et al., 2015; Liu et al., 2015). In our previous studies, based on fractional amplitude of low-frequency fluctuation (fALFF) method, PMS patients had increased fALFF in the whole left hippocampus compared with HCs and altered functional connectivity between the left hippocampus and regions including the medial prefrontal cortex, OFC, precentral cortex (preCC), middle cingulate cortex (MCC) and PCC (Duan et al., 2018; Liao et al., 2017a, b). In comparison with HCs, PMS patients also showed increased regional homogeneity mainly in the bilateral precuneus, left inferior temporal cortex (ITC), right inferior frontal cortex (IFC) and left middle frontal cortex and decreased regional homogeneity in the right anterior cingulate cortex at the luteal phase (Deng et al., 2018). Recently, our team observed thalamocortical dysconnectivity involved in prefrontal cortex and posterior parietal cortex (Liu et al., 2018c).

The human brain is considered one integrative complex network or system, that is consists of multiple subnetworks (Lee et al., 2018; van den Heuvel & Hulshoff Pol, 2010). Graph theory has become a valuable tool in neuroimaging to evaluate the relationship between different brain regions and their organization into large-scale networks (Filippi et al., 2013). Previous researches have suggested that the human brain is organized in a small-world modular structure, the combination of high efficiency and clustering in a small-world architecture that confers high efficiency of information processing at relatively low connection cost (Bullmore & Sporns, 2009; Case et al., 2019; Pereira et al., 2016). Many neuroimaging findings already proved that the small-world network topology of human brain may be disrupted in patients with neurological and psychiatric diseases (Jin et al., 2020), such as Alzheimer's disease (Pereira et al., 2016), schizophrenia (Sun et al., 2018), essential tremor (Benito-Leon et al. 2019), major depressive disorder (Zhang et al., 2011) and social anxiety disorder (Yang et al., 2017). However, it is not clear whether PMS patients present altered brain functional network topology.

Therefore, based on resting-state functional magnetic resonance imaging (fMRI), we tried to explore abnormalities of topological properties of brain functional network in PMS patients by the graph theoretical analysis in this study (Song et al., 2020). We also assessed the relationships between abnormal node properties and PMS-related clinical symptoms. Here, we hypothesized that: 1) all participants including PMS patients and HCs should demonstrate small-world properties; 2) PMS patients should demonstrate altered global topological properties of functional networks and disrupted local network properties compared with those of

HCs; and 3) there may be relationships between the abnormal topological properties and clinical symptoms.

Materials and Methods

Ethics statement

This study was authorized by the local Ethics Committee. All the research procedure for this study were performed in consistent with the Declaration of Helsinki. Prior to the study, we obtained the written informed consent of each participant.

Participants

Twenty PMS patients and twenty-one HCs were accepted by this study. The inclusion criteria of PMS patients were satisfied (Halbreich et al., 2007): 1) the menstrual cycle range: 24–35 days; 2) age: 18–45 years old; 3) right-handedness; 4) in most menstrual cycles, PMS occurred in 2 weeks before menstruation; 5) symptoms were relieved later on the onset of menses and disappeared during most of the mid-follicular phase of the menstrual cycle; 6) the symptoms were refered to abnormality in daily functioning, and caused behavioral, emotional or physical distress; 7) menstrual-relevant periodicity, occurrence during the late luteal phase of cycle (days -5 to -1) and absence during the mid-follicular phase (days $+6$ to $+10$), were documented by repeated observations by the PMS patients based on the daily rating of severity of problems (DRSP) criterion, and the mean score in the late luteal phase was at least 30% greater than the mid-follicular phase; and 8) the symptoms were more than a worsening of another physical chronic or mental disorders.

The exclusion criteria for PMS patients and the experimental paradigm of this study in the Supplementary material (Association AP, 2013; Bao et al., 2004). Twenty-one matched HCs with age, handedness and normal menstrual cycle were evaluated according to the above exclusion criteria.

Data acquisition

Resting-state fMRI data were acquired on a 3.0 T Siemens Magnetom Verio MRI System (Siemens Medical, Erlangen, Germany), using an 8-channel head coil. During the scanning, all participants were asked to stay still and awake, have no thoughts, keep eyes closed. Foam pillows were used to minimize movement between the participant's head and the instrument. Resting-state fMRI data were obtained with a single-shot gradient-recalled echo planar

imaging (EPI) sequence: repetition time (TR) = 2000 ms; echo time (TE) = 30 ms; flip angle (FA) = 90°; field of view (FOV) = 240 mm × 240 mm; slice thickness = 5 mm (no-gap); matrix = 64 × 64; 31 slices and 180 volumes. The total scanning time was about 6 min. High resolution T1-weighted images were then obtained with a volumetric three-dimensional spoiled gradient recall sequence with the parameters as following: TR = 1900 ms; TE = 2.22 ms, FOV = 250 × 250 mm, matrix size: 250 × 250, FA = 9°, slice thickness = 1 mm and 176 slices.

Data preprocessing

The functional image data preprocessing was performed by Data Processing Assistant for Resting-State fMRI (DPARSF) software package (http://rfmri.org/dpabi) based on Statistical Parametric Mapping 12 (SPM 12, http://www.fil.ion.ucl.ac.Uk) on MATLAB platform. The main preprocessing steps: remove the first 5 volumes, slice time correction, head motion correction (discarded the fMRI data with maximum displacement in any cardinal direction > 2.5 mm or head rotation > 2.5°), normalization to the Montreal Neurological Institute (MNI) space (Calhoun et al., 2017) (EPI template with 3 × 3 × 3 mm³ voxel size), nuisance regressions (Friston 24 parameters, cerebrospinal fluid signals, white matter and global mean signals), smoothing (fullwidth at half maximum of 4 mm), detrend and filtering (0.01 < f < 0.1 Hz).

Network construction

In this study, GRETNA 2.0 toolbox (https://www.nitrc.org/projects/gretna) was used to generate the brain network (Wang et al., 2015b). A validated atlas was applied to parceled the brain into 90 regions of interest (Tzourio-Mazoyer et al., 2002). and each region represented a node in brain functional network. Then, the time series of all voxels in each brain region were averaged to obtain the average time series of corresponding brain regions. By calculating the Pearson correlation coefficients between all possible time series pairs of brain regions, a N × N correlation matrix was then constructed for each participant (N = 90) (Wang et al. 2009; Jin et al., 2020). Subsequently, Fisher's r-to-z transformation was further applied to the correlation matrixes (Liu et al., 2017a, b). Since it is suspectable whether self connectivities or negative connectivities is biologically meaningful, the diagonal and negative links were set to zero (Power et al., 2012, 2013). To excluded the weak links that may be spurious and obscure the topology of strong connections, we only analyzed the positive connections in this study (Liang et al., 2012).

Then each correlation matrix was converted into a sparse binarization matrix. Network properties at each sparsity were calculated based on the 90 × 90 binarized matrixes.

Threshold selection

During the binarization process before calculating network properties (Pereira et al., 2016), the minimum sparsity was chosen to ensure that the average degree across all nodes of each threshold-network was greater than 2ln(N) (Jin et al., 2020), and must ensure that each network was fully connected to N nodes (N = 90). The maximum sparsity was chosen to ensure that the small-world attribute of each brain network was greater than 1. This approach guaranteed that all constructed networks from the two comparison groups exhibit the small-worldness and contained the same degree distribution (Rubinov & Sporns, 2010). We chose a large range of sparsity from 20 to 50% with a step of 1% instead of a single threshold to comprehensively evaluate topological properties covering a wide range of sparsity (Wang et al., 2015a). In the binarization, when sparsity was equal to n%, the strongest connections with the highest n% absolute value in the network were set to 1, while other connections were set to 0 (Yang et al., 2017). The details of network properties in the Supplementary material.

Statistical analyses

The two sample t-test was performed to detect differences on the demographic and clinical indicators between the PMS patients and the HCs and the significance level was set at $p < 0.05$.

Because the area under the curves (AUC) are sensitive to the topological alterations of the cerebral disorders and provide a summary measure for topological organization independent from any single threshold selection (Jin et al., 2020; Yang et al., 2017). Group differences between PMS patients and HCs in AUC values of each global and local property across the whole sparsity range, the two sample t-test was applied in this study (Sreenivasan et al., 2019; Yang et al., 2017). All the significance level was set at $p < 0.05$ (uncorrected). In addition, to identify the specific altered functional connectivity pattern in PMS, a statistical significance level of $p < 0.01$ (uncorrected) and network-based statistic (NBS) approaches (Edge: $p = 0.001$; Component: $p < 0.05$; 1000 permutations) (Yang et al., 2017) were applied.

For those network properties showing significant differences between PMS and HCs, Pearson's correlation analysis was used to evaluate potential relationships between the DRSP and important network topological parameters in

Table 1 Clinical and demographic characteristics of the participants

Characteristic	PMS ($N = 20$)	HCs ($N = 21$)	p value[*]
Age (years)	21.85 ± 1.72	21.38 ± 0.86	0.28
HAMA	10.50 ± 6.83	6.81 ± 6.68	0.09
HAMD	13.10 ± 6.54	8.29 ± 3.95	0.01
DRSP	73.47 ± 7.84	35.17 ± 7.90	< 0.001
BMI	18.60 ± 1.71	19.50 ± 1.48	0.08
Menophania (years)	13.75 ± 1.44	13.00 ± 1.09	0.07
Length of menstrual cycle (days)	29.95 ± 1.76	29.80 ± 1.56	0.79
Menstruation (days)	5.60 ± 1.09	5.38 ± 1.11	0.53

Data were expressed as mean ± standard deviation

[*]The p value was obtained by two-sample two-tailed t-test

PMS group (Chen et al., 2020; Jin et al., 2020; Wang et al., 2019). The significant level was set at $p < 0.05$ with the Bonferroni correction (Wang et al., 2019).

Results

Demographic and clinical symptoms results

Twenty PMS patients and twenty-one HCs were accepted by this study. Demographic characteristics of participants are summarized in Table 1. The DRSP and HAMD score in the late luteal phase from HCs was significantly lower than that from PMS patients ($p < 0.05$). There were no significant differences in terms of HAMA, age, BMI, menstruation (days), menophania (years), length of menstrual cycle (days) between the two groups ($p > 0.05$).

Topological difference between PMS and HCs

The graph theory analysis results showed that both PMS and HCs exhibited a small-world organization ($\sigma > 1$) (Fig. 1), while that PMS patients had significantly lower AUC values of γ (aγ) and σ (aσ) at the global level (Fig. 2), and the values of AUC of λ (aλ) between the two groups was found no significant differences (Fig. 2). The PMS patients demonstrated no significant differences of the AUC of Eg ($p > 0.05$) and Eloc ($p > 0.05$) compared with HCs group (Fig. 3). The original weighting matrix and the mean binary adjacency matrix of HCs and PMS patients were obtained when the correlation threshold $s = 0.32$ (Fig. 4).

Significant differences of the AUC of node properties between groups are shown in Fig. 5. Compared with HCs, PMS patients had increased AUC values of DC in the left preCC, right inferior orbitofrontal cortex (iOFC), and decreased in the right posterior cingulate cortex (PCC),
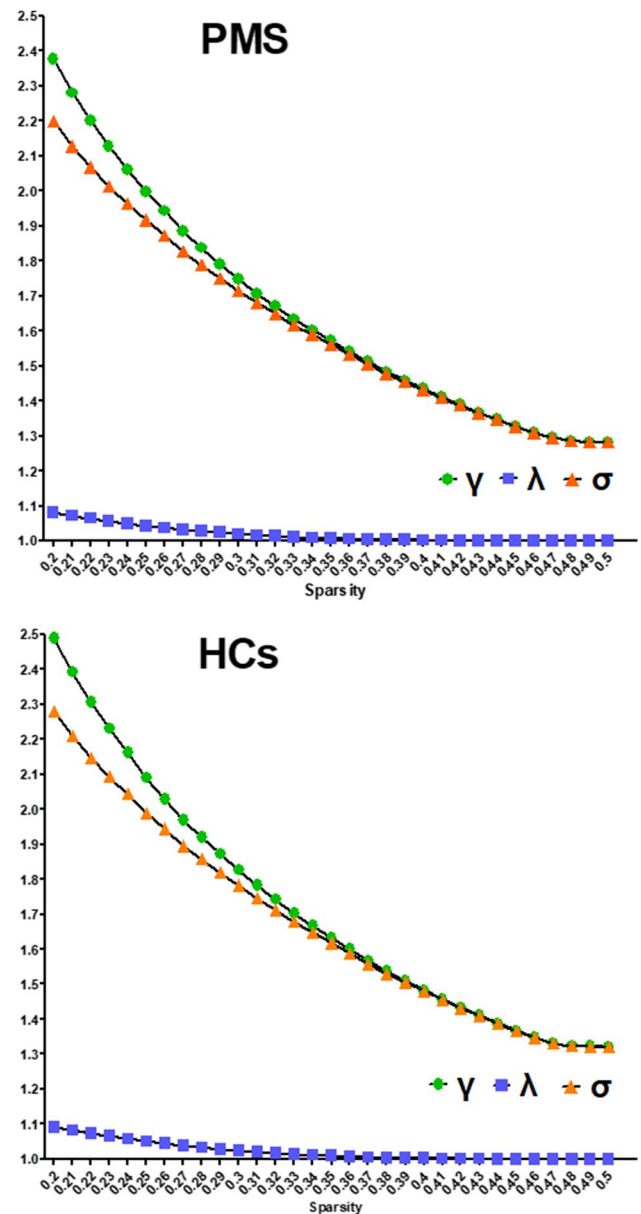

Fig. 1 In the defined threshold range, PMS and HCs groups showed γ and σ substantially higher than 1, and λ approximately equal to 1, suggesting that all participants satisfied the typical feature of the small-world properties

right angular gyrus (ANG), bilateral precuneus (preCUN) and right thalamus (THA) (Fig. 5A). In PMS patients, the AUC values of Ei (aEi) increased in the left preCC and inferior orbitofrontal cortex (iOFC), but decreased in the right PCC (Fig. 5B), and the AUC values of NLp performed the contrary to the aEi (Fig. 5C). The AUC of NCp and NLe both decreased in the bilateral PCC, ANG, putamen (PUT), pallidum (PAL) and THA (Fig. 5D, E).
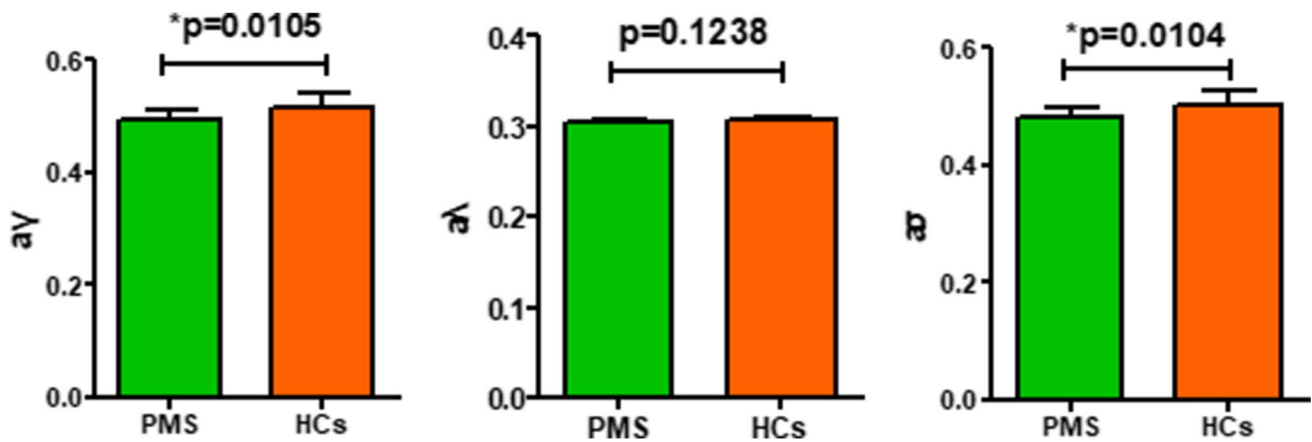
Fig. 2 The comparisons of aσ, aγ and aλ between the PMS patients and HCs of brain functional networks. Error bars represent standard deviation. * indicates statistical significant difference

Fig. 3 No significant differences of aE_g and aE_{loc} between the PMS patients and HCs. Error bars represent standard deviation. * indicates statistical significant difference
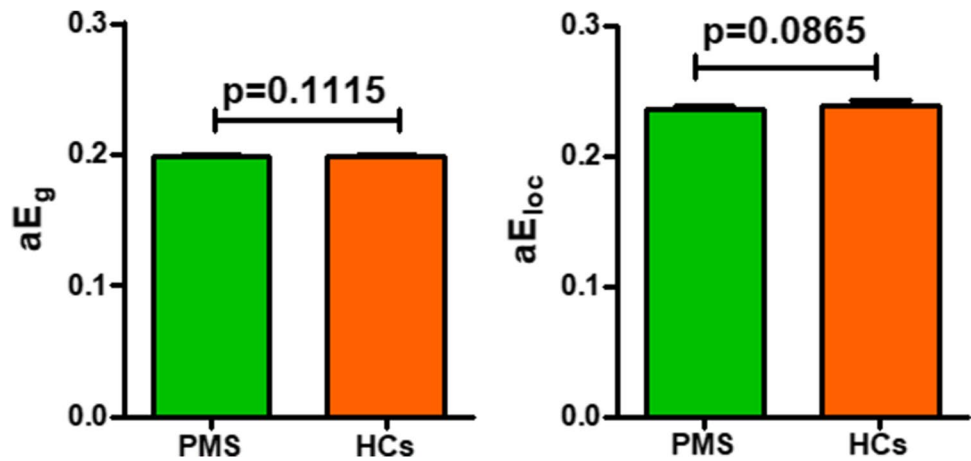
As presented in Fig. 6, PMS patients had abnormality of connected network including 11 edges, and the components were mainly associated with the supplementary motor area (SMA), PCC, ANG, PUT and PAL and THA (p < 0.01, uncorrected).

Relationship between network measures and clinical symptoms

Only one significant relationship between the altered topological properties and clinical symptoms was observed, related to the negative correlation between the AUC of NLe in the left PCC and DRSP scores (r = -0.6440, $p = 0.0022$) in Fig. 7.

Discussion

The main findings were identified: 1) at the global level, both of the PMS and HCs groups exhibited small-world properties, and the values of σ and γ exhibited significantly decreased of PMS patients; 2) at the local level, there were significantly altered in node attributes in several brain regions of PMS patients, mainly related to the areas of pre-CUN, PCC, ANG, PUT, PAL and THA; 3) The PMS group revealed altered specific functional connections; and 4) the negative correlation between the AUC values of NLe in the left PCC and DRSP scores was discovered in PMS patients.

It was evidenced that functional connections of brain networks are constructed in a well-organized small-world manner (Rubinov & Sporns, 2010), and small world networks featured as high clustering and low path lengths (Case et al., 2019), which are important to ensure a high level of segregation and integration of information within the overall network (Sreenivasan et al., 2019). The segregation in
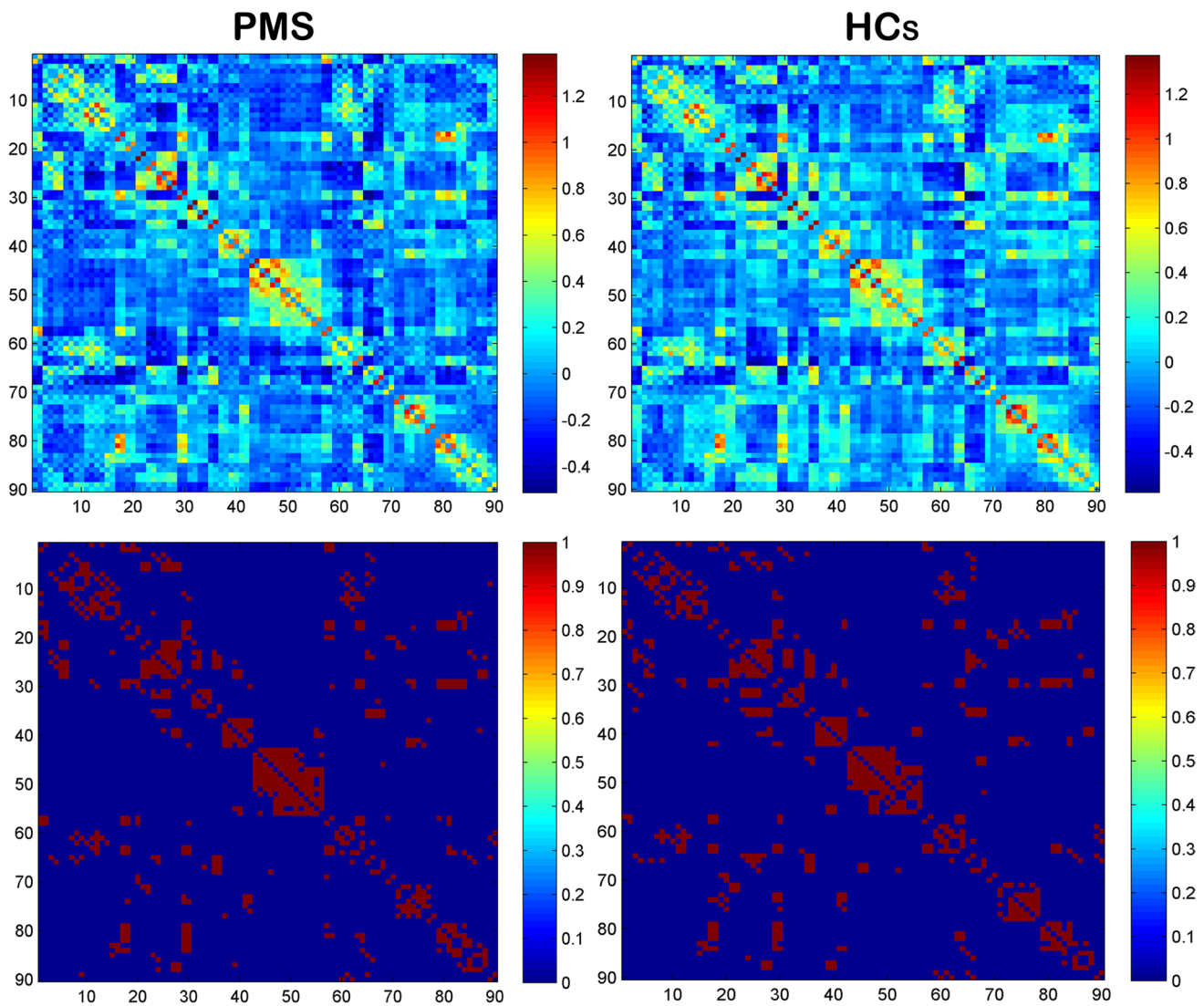
Fig. 4 The original weighting matrix and the mean binary adjacency matrices in PMS patients and HCs at a correlation threshold of 0.32

the network can be measured by γ, while the global functional integration is usually measured by λ (Rubinov & Sporns, 2010). In this study, both PMS patients and HCs have a small world organization of brain functional networks (σ > 1), PMS patients exhibited significantly reduced σ and γ, and no significant alterations of λ between the groups, but a trend was observed where the PMS patients tended to have decrease λ values compared to HCs (Case et al., 2019). This similar changes has been observed in brain functional network in other diseases, such as end-stage renal disease (Jin et al., 2020) and optic neuritis (Song et al., 2020; Wang et al., 2019). The decreased γ was speculated that a loss in optimal modular information processing (functional segregation) in PMS patients (Sreenivasan et al., 2019). Therefore, alternations of the small-worldness of networks may

be relevant to the differences of brain function between HCs and PMS patients.

In this study, several regions showed significantly altered nodal properties in PMS patients compared to HCs, predominantly including: the PCC, preCUN and ANG. These changed brain regions are the posterior nodes in the DMN (Wang et al., 2015a; Wu et al., 2020). PCC has been evidenced to be involved in the evaluation of self-associated sensations (Liu et al., 2018b). The preCUN is engaged in processing of sensorimotor and self-related mental representations during rest (Cavanna & Trimble, 2006). It has been reported that the ANG is associated with self-referential processing, and plays a crucial role in countering anxiety and negative emotions. Altered structural covariance between the ANG, PCC and preCUN was found in major depressive disorder (Wu et al., 2016a, b). Moreover, the DRSP score
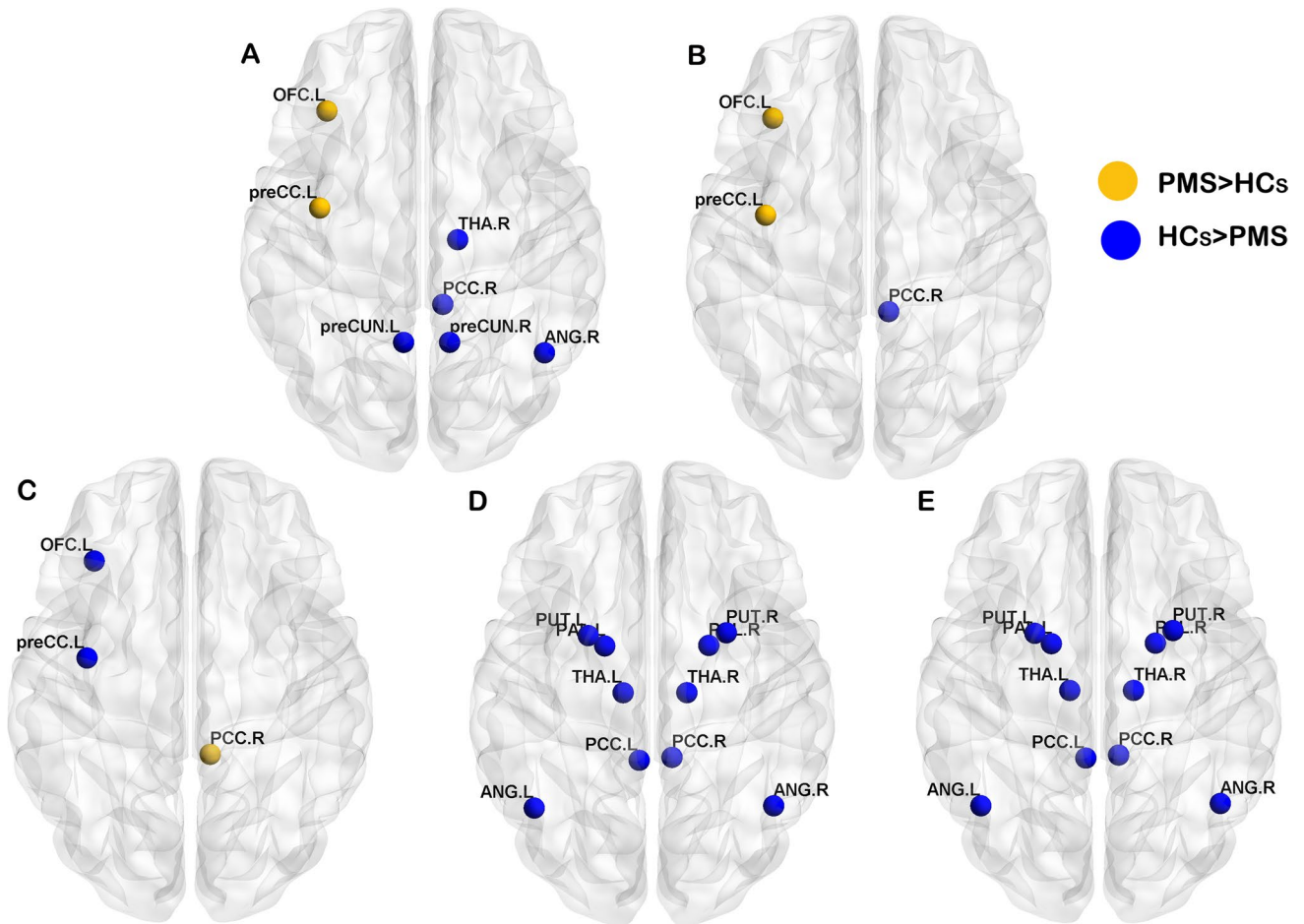
Fig. 5 Brain regions with significant differences of aDC (A), aE$_i$ (B), aNL$_p$ (C), aNC$_p$ (D) and aNL$_e$ (E) among participants in PMS patients and HCs. Yellow sphere demonstrated that nodal metrics in PMS group were increased compared with HCs group. Blue sphere showed that nodal network measures in PMS group were decreased relative to HCs group

significantly negatively correlated with the values of aNLe of PCC in PMS group. Based on these findings in our study, we thereby infer that the abnormalities of node attributes in

the PCC, preCUN and ANG could be associated with disturbances of self-referential, sensations and emotion regulation.
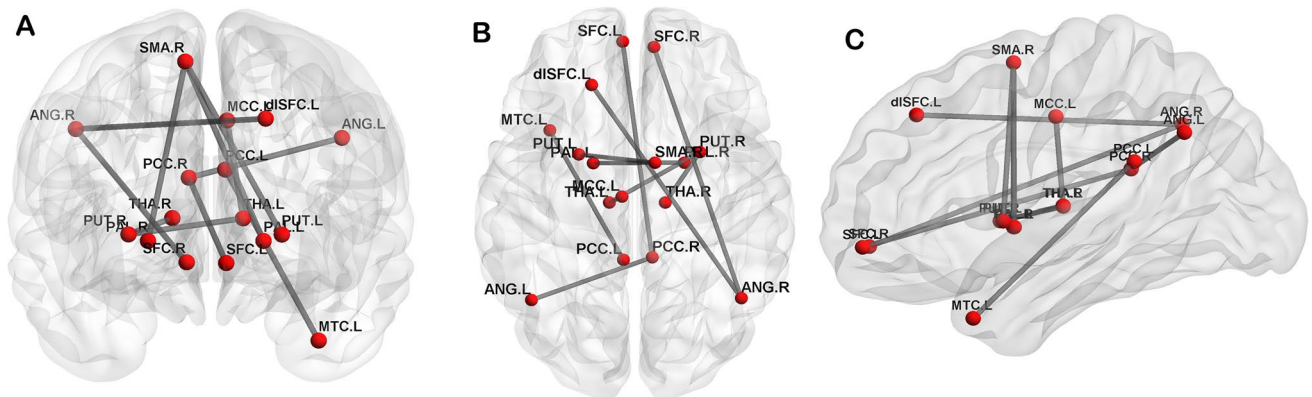

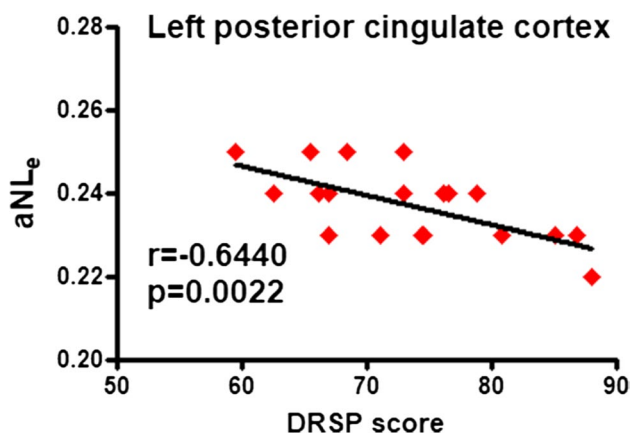**Fig. 6** The altered connections between the PMS patients and HCs

Fig. 7 Negative correlation between the values of aNLe in the left PCC and DRSP scores in the PMS patients

Our study detected functional abnormalities of THA in PMS patients, relevant with decreased THA nodal metrics and THA-related connectivities to the MCC and PUT. The THA is one of the most important sensory transform stations. In the THA, various sensory pathways which including cognitive, visceral and arousal functions exchange neurons, and then project to the cerebral cortex (Van der Werf et al., 2002). Previous studies discovered that the altered nodal attributes of THA were closely related to social anxiety disorder, schizophrenia and functional dyspepsia (Liu et al., 2008, 2013; Yang et al., 2017). Several studies indicated the MCC as important hubs of the homeostatic afferent and emotional-arousal networks, mainly evaluates the importance of emotional regulation and visceral stimulation (Elsenbruch et al., 2010). PUT is known to be related to sensory aspects of regulating negative emotions. and several mood disorders, such as, depression and bipolar disorder (Liu et al., 2015). Hence, we speculate that PMS patients may be more sensitive to unpleasant situations and perception of visceral sensations and even negative emotion regulation, partly associated with altered topological properties of the THA, MCC and PUT.

Limitations

This study contains several limitations. First, this study only concerned the alterations of brain functional networks in PMS patients, the combined analysis of structural and functional networks may be more effectively identify brain abnormalities in patients with PMS patients in future studies. Second, hormone level of participants was not evaluated in this study.

Conclusion

In this study, we examined the topological properties of functional networks between PMS patients and HCs using graph theory. Compared with HCs, PMS patients had disturbed global and local properties of nodes and connections involved in emotional processing, visceral sensations and cognition. Furthermore, we found a significant negatively correlation between the aNLe values of the left PCC and the DRSP score in PMS patients. We expect that graph theory analysis may be helpful in providing new evidence of network disruption of brain function in PMS patients and improving our understanding of neural mechanisms of PMS.

Abbreviations PMS: Premenstrual syndrome; HCs: Healthy controls; HAMA: Hamilton anxiety scale; HAMD: Hamilton depression scale; DRSP: Daily record of severity of problems; BMI: Body mass index; C_p: Clustering coefficients; L_p: Characteristic path lengths; γ: Normalized clustering coefficients; λ: Normalized characteristic path lengths; σ: Small-worldness; E_g: Network global efficiency; E_{loc}: Network local efficiency; DC: Degree centrality; E_i: Nodal efficiency; NL_e: Nodal local efficiency; NL_p: Node characteristic path length; NC_p: Node clustering coefficient; The symbol "a" stands for the areas under the curves (AUC) of the topological metrics (Cp, Lp, γ, λ, σ, Eg, Eloc, DC, Ei, NLe, NLp, NCp); R: Right; L: Left; preCC: Precentral cortex; dlSFC: Dorsolateral superior frontal cortex; OFC: Orbitofrontal cortex; SMA: Supplementary motor area; SFC: Superior frontal cortex; MCC: Middle cingulate cortex; PCC: Posterior cingulate cortex; ANG: Angular gyrus; preCUN: Precuneus; PUT: Putamen; PAL: Pallidum; THA: Thalamus; STC: Superior temporal cortex; MTC: Middle temporal cortex

Declarations

Conflict of interest The authors declare that there is no conflict of interest.

Reference

Association, A. P. (2013). Diagnostic and Statistical Manual of Mental Disorders, 5th ed. Washington, DC: American Psychiatric Press (3), 275–277.

Bao, A. M., Ji, Y. F., Van Someren, E. J., Hofman, M. A., Liu, R. Y., & Zhou, J. N. (2004). Diurnal rhythms of free estradiol and cortisol

during the normal menstrual cycle in women with major depression. *Hormones and Behavior, 45*(2), 93–102.

Benito-Leon, J., Sanz-Morales, E., Melero, H., Louis, E. D., Romero, J. P., Rocon, E., et al. (2019). Graph theory analysis of resting-state functional magnetic resonance imaging in essential tremor. *Human Brain Mapping, 40*(16), 4686–4702.

Bu, L., Lai, Y., Deng, Y., Xiong, C., Li, F., Li, L., et al. (2019). Negative Mood Is Associated with Diet and Dietary Antioxidants in University Students During the Menstrual Cycle: A Cross-Sectional Study from Guangzhou, China. *Antioxidants (basel), 9*(1), 23.

Bullmore, E., & Sporns, O. (2009). Complex brain networks: Graph theoretical analysis of structural and functional systems. *Nature Reviews Neuroscience, 10*(3), 186–198.

Calhoun, V. D., Wager, T. D., Krishnan, A., Rosch, K. S., Seymour, K. E., Nebel, M. B., et al. (2017). The impact of T1 versus EPI spatial normalization templates for fMRI data analyses. *Human Brain Mapping, 38*(11), 5331–5342.

Case, M., Shirinpour, S., Vijayakumar, V., Zhang, H., Datta, Y., Nelson, S., et al. (2019). Graph theory analysis reveals how sickle cell disease impacts neural networks of patients with more severe disease. *Neuroimage Clinical, 21*, 101599.

Cavanna, A. E., & Trimble, M. R. (2006). The precuneus: A review of its functional anatomy and behavioural correlates. *Brain, 129*(Pt 3), 564–583.

Chen, H., Sheng, X., Luo, C., Qin, R., Ye, Q., Zhao, H., et al. (2020). The compensatory phenomenon of the functional connectome related to pathological biomarkers in individuals with subjective cognitive decline. *Translational Neurodegeneration, 9*(1), 21.

De Bondt, T., Smeets, D., Pullens, P., Van Hecke, W., Jacquemyn, Y., & Parizel, P. M. (2015). Stability of resting state networks in the female brain during hormonal changes and their relation to premenstrual symptoms. *Brain Research, 1624*, 275–285.

Deng, D., Pang, Y., Duan, G., Liu, H., Liao, H., Liu, P., et al. (2018). Larger volume and different functional connectivity of the amygdala in women with premenstrual syndrome. *European Radiology, 28*(5), 1900–1908.

Duan, G., Liu, H., Pang, Y., Liu, P., Liu, Y., Wang, G., et al. (2018). Hippocampal fractional amplitude of low-frequency fluctuation and functional connectivity changes in premenstrual syndrome. *Journal of Magnetic Resonance Imaging, 47*(2), 545–553.

Elsenbruch, S., Rosenberger, C., Enck, P., Forsting, M., Schedlowski, M., & Gizewski, E. R. (2010). Affective disturbances modulate the neural processing of visceral pain stimuli in irritable bowel syndrome: An fMRI study. *Gut, 59*(4), 489–495.

Filippi, M., van den Heuvel, M. P., Fornito, A., He, Y., Hulshoff Pol, H. E., Agosta, F., et al. (2013). Assessment of system dysfunction in the brain through MRI-based connectomics. *Lancet Neurology, 12*(12), 1189–1199.

Halbreich, U., Backstrom, T., Eriksson, E., O'Brien, S., Calil, H., Ceskova, E., et al. (2007). Clinical diagnostic criteria for premenstrual syndrome and guidelines for their quantification for research studies. *Gynecological Endocrinology, 23*(3), 123–130.

Jin, M., Wang, L., Wang, H., Han, X., Diao, Z., Guo, W., et al. (2020). Altered resting-state functional networks in patients with hemodialysis: a graph-theoretical based study. *Brain Imaging and Behavior, 15*(2), 833–845.

Le, J., Thomas, N., & Gurvich, C. (2020). Cognition, The Menstrual Cycle, and Premenstrual Disorders: A Review. *Brain Sciences, 10*(4), 198.

Lee, L. C., Chen, Y. H., Lin, C. S., Li, W. C., Low, I., Tu, C. H., et al. (2018). Unaltered intrinsic functional brain architecture in young women with primary dysmenorrhea. *Science and Reports, 8*(1), 12971.

Liang, X., Wang, J., Yan, C., Shu, N., Xu, K., Gong, G., et al. (2012). Effects of different correlation metrics and preprocessing factors on small-world brain functional networks: a resting-state functional MRI study. *PLoS ONE, 7*(3), e32766.

Liao, H., Duan, G., Liu, P., Liu, Y., Pang, Y., Liu, H., et al. (2017a). Altered fractional amplitude of low frequency fluctuation in premenstrual syndrome: A resting state fMRI study. *Journal of Affective Disorders, 218*, 41–48.

Liao, H., Pang, Y., Liu, P., Liu, H., Duan, G., Liu, Y., et al. (2017b). Abnormal Spontaneous Brain Activity in Women with Premenstrual Syndrome Revealed by Regional Homogeneity. *Frontiers in Human Neuroscience, 11*, 62.

Liu, F., Wang, Y., Li, M., Wang, W., Li, R., Zhang, Z., et al. (2017a). Dynamic functional network connectivity in idiopathic generalized epilepsy with generalized tonic-clonic seizure. *Human Brain Mapping, 38*(2), 957–973.

Liu, P., Li, R., Bao, C., Wei, Y., Fan, Y., Liu, Y., et al. (2018a). Altered topological patterns of brain functional networks in Crohn's disease. *Brain Imaging and Behavior, 12*(5), 1466–1478.

Liu, P., Wei, Y., Fan, Y., Li, R., Liu, Y., Wang, G., et al. (2018b). Altered brain structure in women with premenstrual syndrome. *Journal of Affective Disorders, 229*, 239–246.

Liu, P., Wei, Y., Liao, H., Fan, Y., Li, R., Feng, N., et al. (2018c). Thalamocortical dysconnectivity in premenstrual syndrome. *Brain Imaging and Behavior, 13*(3), 717–724.

Liu, P., Zeng, F., Zhou, G., Wang, J., Wen, H., von Deneen, K. M., et al. (2013). Alterations of the default mode network in functional dyspepsia patients: A resting-state fmri study. *Neurogastroenterology and Motility, 25*(6), 382–388.

Liu, Q., Li, R., Zhou, R., Li, J., & Gu, Q. (2015). Abnormal Resting-State Connectivity at Functional MRI in Women with Premenstrual Syndrome. *PLoS ONE, 10*(9), e0136029.

Liu, Q., Wang, Y., van Heck, C. H., & Qiao, W. (2017b). Stress reactivity and emotion in premenstrual syndrome. *Neuropsychiatric Disease and Treatment, 13*, 1597–1602.

Liu, Y., Liang, M., Zhou, Y., He, Y., Hao, Y., Song, M., et al. (2008). Disrupted small-world networks in schizophrenia. *Brain, 131*(4), 945–961.

Pereira, J. B., Mijalkov, M., Kakaei, E., Mecocci, P., Vellas, B., Tsolaki, M., et al. (2016). Disrupted Network Topology in Patients with Stable and Progressive Mild Cognitive Impairment and Alzheimer's Disease. *Cerebral Cortex, 26*(8), 3476–3493.

Power, J. D., Barnes, K. A., Snyder, A. Z., Schlaggar, B. L., & Petersen, S. E. (2012). Spurious but systematic correlations in functional connectivity MRI networks arise from subject motion. *NeuroImage, 59*(3), 2142–2154.

Power, J. D., Schlaggar, B. L., Lessov-Schlaggar, C. N., & Petersen, S. E. (2013). Evidence for hubs in human functional brain networks. *Neuron, 79*(4), 798–813.

Quintana-Zinn, F. A., Whitcomb, B. W., Ronnenberg, A. G., Bigelow, C., Houghton, S. C., & Bertone-Johnson, E. R. (2017). Premenstrual Symptom Patterns and Behavioral Risk Factors in Young Women: A Cross-Sectional Study. *Journal of Women's Health (2002), 26*(10), 1099–1105.

Rubinov, M., & Sporns, O. (2010). Complex network measures of brain connectivity: Uses and interpretations. *NeuroImage, 52*(3), 1059–1069.

Ryu, A., & Kim, T. H. (2015). Premenstrual syndrome: A mini review. *Maturitas, 82*(4), 436–440.

Song, K., Li, J., Zhu, Y., Ren, F., Cao, L., Shao, Y., et al. (2021). Altered small-world functional network topology in patients with optic neuritis: A resting-state fMRI study. Dis Markers, 2021, 9948751.

Sreenivasan, K., Mishra, V., Bird, C., Zhuang, X., Yang, Z., Cordes, D., et al. (2019). Altered functional network topology correlates with clinical measures in very early-stage, drug-naive Parkinson's disease. *Parkinsonism & Related Disorders, 62*, 3–9.

Sun, Y., Collinson, S. L., Suckling, J., & Sim, K. (2018). Dynamic Reorganization of Functional Connectivity Reveals Abnormal Temporal Efficiency in Schizophrenia. *Schizophrenia Bulletin, 45*(3), 659–669.

Tolossa, F. W., & Bekele, M. L. (2014). Prevalence, impacts and medical managements of premenstrual syndrome among female students cross-sectional study in college of health sciences. *BMC Women's Health, 14*, 52.

Tzourio-Mazoyer, N., Landeau, B., Papathanassiou, D., Crivello, F., Etard, O., Delcroix, N., et al. (2002). Automated anatomical labeling of activations in SPM using a macroscopic anatomical parcellation of the MNI MRI single-subject brain. *NeuroImage, 15*(1), 273–289.

van den Heuvel, M. P., & Hulshoff Pol, H. E. (2010). Exploring the brain network: A review on resting-state fMRI functional connectivity. *European Neuropsychopharmacology, 20*(8), 519–534.

Wang, J., Wang, L., Zang, Y., Yang, H., Tang, H., Gong, Q., et al. (2009). Parcellation-dependent small-world brain functional networks: A resting-state fMRI study. *Human Brain Mapping, 30*(5), 1511–1523.

Wang, J., Wang, X., He, Y., Yu, X., Wang, H., & He, Y. (2015a). Apolipoprotein E ε4 modulates functional brain connectome in Alzheimer's disease. *Human Brain Mapping, 36*(5), 1828–1846.

Wang, J., Wang, X., Xia, M., Liao, X., Evans, A., & He, Y. (2015b). GRETNA: A graph theoretical network analysis toolbox for imaging connectomics. *Frontiers in Human Neuroscience, 9*, 386.

Wang, Y., Zheng, L., Liu, Y., Ye, Y., Luo, S., Lu, G., et al. (2019). The gut microbiota-inflammation-brain axis in end-stage renal disease: Perspectives from default mode network. *Theranostics, 9*(26), 8171–8181.

Wu, H., Sun, H., Wang, C., Yu, L., Li, Y., Peng, H., et al. (2016a). Abnormalities in the structural covariance of emotion regulation networks in major depressive disorder. *Journal of Psychiatric Research, 84*, 237–242.

Wu, M., Liang, Y., Wang, Q., Zhao, Y., & Zhou, R. (2016b). Emotion Dysregulation of Women with Premenstrual Syndrome. *Science and Reports, 6*(38501), 1–10.

Wu, Y., Wang, C., Qian, W., Yu, L., Xing, X., Wang, L., et al. (2020). Disrupted default mode network dynamics in recuperative patients of herpes zoster pain. *CNS Neuroscience & Therapeutics, 00*, 1–10.

Yang, X., Liu, J., Meng, Y., Xia, M., Cui, Z., Wu, X., et al. (2017). Network analysis reveals disrupted functional brain circuitry in drug-naive social anxiety disorder. *NeuroImage, 190*, 213–223.

Van der Werf, Y. D., Witter, M. P., & Groenewegen, H. J. (2002). The intralaminar and midline nuclei of the thalamus. Anatomical and functional evidence for participation in processes of arousal and awareness. *Brain Research Reviews, 39*(2–3), 107–140.

Zhang, J., Wang, J., Wu, Q., Kuang, W., Huang, X., He, Y., et al. (2011). Disrupted brain connectivity networks in drug-naive, first-episode major depressive disorder. *Biological Psychiatry, 70*(4), 334–342.